ROMAI J., **4**, 2(2008), 146–168

MATHEMATICAL AND NUMERICAL MODEL OF ROCK/CONCRETE MECHANICAL BEHAVIOR IN A MULTI-PLANE FRAMEWORK

Seyed Amirodin Sadrnejad

Faculty of Civil Engineering, K.N.Toosi University of Technology,

Tehran, Iran

sadrnejad@kntu.ac.ir

Abstract Among the various mathematical and numerical simulating models of plane concrete, the multi-planes models have an excellent position. These models are not as complicated as microscopic models, such as discrete particles models, and do not have the shortcomings of macroscopic models based on the stress or strain invariants. The object of this study is the presentation of a developed multi-planes damage based model of plane concrete through a 3D finite elements code to show its abilities in crack/damage analysis of actual rock/concrete/concrete structures such as a double curvature arch dam. The proposed code not only is able to predict the crack line, but also determines which combination of loading conditions occurs on damaged multi-planes.

The presented multi-plane based model is capable of seeing both dynamic and elastoplastic behavior of rock/concretes and concrete, with a particular focus on semi-micromechanical behavior of geo-materials. The constitutive equations of this model is derived within the context of elastic behavior of the whole medium and plastic sliding of interfaces of predefined multi-plane, not missing the directional effects. The formulation incorporates explicitly the notion of the preferred direction, with a description of the medium as an assembly of discrete polyhedron elements that support the overall applied loads through contact friction and cohesion. The overall mechanical response ideally may be described on the basis of micro-mechanical behavior of discrete polyhedron elements interconnections.

According to this model, the overall deformation of any small part of the medium is composed of total elastic response and an appropriate summation of sliding, separation/closing phenomenon under the current effective normal and shear stresses on sampling planes. These assumptions adopt overall sliding, separation/closing of inter-granular points of grains included in one structural

unit (discrete polyhedron elements) are summed up and contributed as the result of sliding, separation/closing surrounding boundary planes. This simply implies yielding/failure or even ill-conditioning, bifurcation response damage and fragmentation phenomena to be possible over any of the randomly oriented sampling planes. Consequently, plasticity control such as yielding should be checked at each of the planes and those of the planes that are sliding will contribute to plastic deformation. Therefore, the geo-material mass has an infinite number of yield functions usually one for each of the planes in the physical space. Compact and isotropic synthetic media are generated automatically and are used to investigate the mechanical behavior of these low-porosity materials. In the case of micro-mechanics, the model considers the two-phase, aggregate and cement medium, at a macroscopic scale.

The proposed multi-plane based model is capable of predicting the behavior of materials under different orientation of bedding plane, history of strain progression during the application of any stress/strain paths, based on five types of planar behavior of sampling planes. Validity of the proposed model is investigated through a few standard benchmark examples.

Keywords: mechanics of geo-materials, micromechanical behavior.

2000 MSC: 74L05, 74L10.

1. INTRODUCTION

A survey through the published scientific papers deals with the object of constitutive modeling of geo-materials. All models are categorized into two main classes: continuous and discontinuous models. In the first class, it is postulated that the overall mass of material is continuous and no crack/rupture/gap or fracture are allowed. On the other hand, in the last class, the material is assumed to act as an assemblage of the discrete particles, which can affect on the movements of each others. In turn, the continuous models consist of two large groups: macroscopic models in the context of damage and plasticity theory or combination of both and mesoscopic models such as micro-plane or multi-laminate models. However discontinuous models are placed into one category as microscopic models such as discrete particle models. The macroscopic models concern the definition of relation between stress and strain tensors (structural scale) and the meso-scopic models deal with the same object but in a different way. The later captures this goal by assigning of the relation

between the stress and strain components of the different planes with prescribed orientations called "micro or multi planes". Finally, the microscopic models concern the discrete particle models consisting of convex polygons that are able to withstand a limited cohesion (granular scale). A description of contacts of particles as well as a bond formulation between them could lead to forces induced by particle movements. These forces are inserted into the equations of motion, which are solved numerically based on the discrete element methodology.

A technique for modeling degraded planes and enabling conventional stress/strain analysis of a multidirectional laminate through rock/concrete media including different mechanical behavior aspects, such as the induced anisotropy, softening and strength reduction, and the localization distribution at any location is presented. For the analysis, degraded planes are replaced by a continuum model with a lower stiffness matrix. The degree of stiffness reduction is estimated by acoustic emission like method by considering semi-micromechanics effective stiffness of a laminate having degraded sliding or opening through change of properties.

Given the intrinsic oriented nature of geo-material fabric similar to rock/concrete, it is important to include the effect of anisotropy in a rational way. In this respect, the major obstacles, are our ability to properly define the spatial and temporal variations of the material properties, deformability, hardening/softening and boundary conditions. The value of a model lies primarily in its ability to capture the basic trends in the material behavior and thereby provide a more realistic representation of the problem.

2. FROM SLIP PLANES TO MICRO PLANES

The basic idea, namely that of the constitutive material behavior as a relationship between strain and stress tensors which can be "assembled" from the behavior of material, on the planes with different orientations within the material such as slip planes, micro cracks, particle contacts etc., might be traced back to the failure envelopes of Mohr (1900) and the "slip theory of plasticity" of G. I. Taylor (1938) who was the first that implemented this mentioned theory for modeling the behavior of polycrystalline metals. Taylor's idea was

formulated in detail by Batdorf and Budiansky (1949). This theory was soon recognized as the most realistic constitutive model for plastic-hardening metals. It was refined in a number of subsequent works (e.g. Lin and Ito 1965, 1966, Kröner 1961, Budianski and Wu 1962, Hill, 1965, 1966, Rice, 1970). It was used in arguments about the physical origin of strain hardening, and was shown to allow easy modeling of anisotropy as well as the vertex effects for loading increment to the side of a radial path in stress space. All formulations considered that only the inelastic shear strains ('slips'), with no inelastic normal strain, were taking place on what is now called the 'micro-planes'. The theory was also adapted to anisotropic rocks and soils under the name "multi laminate model" (Zienkiewicz and Pande 1977, Pande and Sharma 1981, 1982; Pande and Xiong 1982).

In these works there is a common assumption that the planes of plastic slip in the material (in those studies called the 'slip-planes' and in this article called the 'micro-planes') are constrained statically to the stress ('macro-stress') tensorσ_{ij} (i.e. the stress vector on each 'micro-plane' was the projection ofσ_{ij}). The static constraint formulation was extensively used under the name of slip theory for metals or multi-laminate theory for anisotropic rocks until the first application of this theory by Bažant and Gambarova in 1984 and Bažant in 1984, to continuum damage mechanics and cohesive-frictional materials, who, for the first time, changed its name from slip theory or multi-laminate theory to micro-plane theory.

In all multi-plane models, such as slip-planes or multi-laminate models, first the macro-stress tensor was projected on the micro-planes and then by introducing on-plane constitutive laws, the micro-strain components were calculated and finally the macro-strain tensor was identified by superposition of on-plane micro-strain components upon any of sampling plane transformation matrix obtained through direction cosines of sampling points on the surface of a unit sphere

$$\int_{\Omega} f\left(x,y,z\right) d\Omega = 4\pi \sum_{p} W_p f\left(x_p, y_p, z_p\right). \tag{1}$$

Now consider the stress tensor σ_{ij} in the macro-level state at the center of the unit sphere as always is used in the micro-plane models. Then, we are going to project this tensor on the planes, which are tangent to the surface of the sphere at the prescribed points. The number and position of these points are determined depending on the numerical integration formulation which was elected for doing integration of an arbitrary function over the surface of the unit sphere. It is worth noting that the origin of the initiation and propagation of the multi-plane models including micro-plane or multi-laminate models are used as this mathematical numerical formulation for integration. Here, for this job, we use a precise formulation of 26 integration points. In Table 1, direction cosines and weights of the integration points and in fig. 1, their positions on the surface of the unit sphere are shown. If we project the stress tensor to the surface of the sphere, we have

$$\begin{gathered}\sigma_N = N_{ij}\sigma_{ij},\ N_{ij} = n_i n_j,\\ \sigma_M = M_{ij}\sigma_{ij},\ M_{ij} = \left(m_i n_j + m_j n_i\right)/2,\\ \sigma_L = L_{ij}\sigma_{ij},\ L_{ij} = \left(l_i n_j + l_j n_i\right)/2\end{gathered} \tag{2}$$

where $n_i, \quad i = 1,2,3$ are the direction cosines of the unit vector normal to the plane and $m_i, l_i, \quad i = 1,2,3$ are the direction cosines of two orthogonal unit vectors tangent to the plane.

Direction Cosines			Weight	Direction cosins			Weight
ℓ_i	m_i	n_i	W_i	ℓ_i	m_i	n_i	W_i
$\sqrt{1/3}$	$\sqrt{1/3}$	$\sqrt{1/3}$	27/840	$\sqrt{1/3}$	$-\sqrt{1/3}$	$\sqrt{1/3}$	27/840
$-\sqrt{1/3}$	$\sqrt{1/3}$	$\sqrt{1/3}$	27/840	$-\sqrt{1/3}$	$-\sqrt{1/3}$	$\sqrt{1/3}$	27/840
$\sqrt{1/2}$	$\sqrt{1/2}$	0.0	32/840	$-\sqrt{1/2}$	$\sqrt{1/2}$	0.0	32/840
$\sqrt{1/2}$	0.0	$\sqrt{1/2}$	32/840	$-\sqrt{1/2}$	0.0	$\sqrt{1/2}$	32/840
0.0	$-\sqrt{1/2}$	$\sqrt{1/2}$	32/840	0.0	$+\sqrt{1/2}$	$\sqrt{1/2}$	32/840
1.0	0.0	0.0	40/840	0.0	1.0	0.0	40/840
0.0	0.0	1.0	40/840				

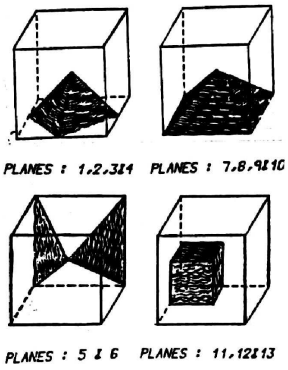

Fig. 1. Definition of micro-planes.

For convenience of calculations, one of the unit vectors tangent to the plane is assumed to be horizontal (parallel to $x - y$ plane). For instance, the pro-

jection of the stress tensor on the plane number 1 results in

$$\sigma_N = \frac{1}{3}\left(\sigma_x + \sigma_y + \sigma_z\right) + \frac{2}{3}\left(\tau_{xy} + \tau_{yz} + \tau_{zx}\right),$$
$$\sigma_M = \frac{1}{\sqrt{6}}\left(-\sigma_x + \sigma_y + \tau_{yz} - \tau_{zx}\right), \tag{3}$$
$$\sigma_L = \frac{1}{\sqrt{18}}\left(\sigma_x + \sigma_y - 2\sigma_z + 2\tau_{xy} - \tau_{yz} - \tau_{zx}\right),$$

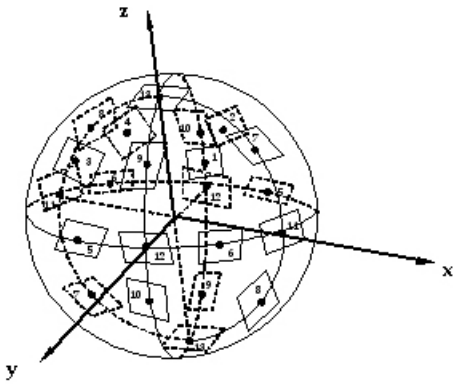

Fig. 2. Position of integration points on the unit sphere' surface.

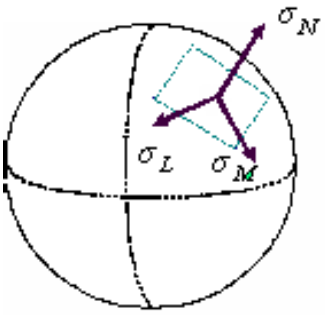

Fig. 3. Projection of stress tensor on the surface of unit sphere.

In order to obtain the original stress tensor from its projections on the micro-planes, first necessary to transfer every stress vector on the micro-plane

from local coordinate to the global coordinate system and then we can add them up according to their weightings. Obviously, the result must be equal to numerical integration of the on-plane stress tensor. This numerical integration is a crucial step in the construction of any micro-plane model. In order to transfer every micro-stress vector to the macro state the following transition matrix can be written

$$T_p = \begin{bmatrix} N_{11} & M_{11} & L_{11} \\ N_{22} & M_{22} & L_{22} \\ N_{33} & M_{33} & L_{33} \\ N_{12} & M_{12} & L_{12} \\ N_{23} & M_{23} & L_{23} \\ N_{13} & M_{13} & L_{13} \end{bmatrix}_p . \tag{4}$$

The subscript p denotes any specified micro-plane. So, we can write

$$\hat{\sigma}_p = T_p.\bar{\sigma} = T_p.\sigma : N_p, \tag{5}$$

$$\sigma : N_p = \begin{bmatrix} n_1 & n_2 & n_3 \\ m_1 & m_2 & m_3 \\ l_1 & l_2 & l_3 \end{bmatrix} \begin{bmatrix} \sigma_x & \tau_{xy} & \tau_{xz} \\ \tau_{xy} & \sigma_y & \tau_{yz} \\ \tau_{xz} & \tau_{yz} & \sigma_z \end{bmatrix} \begin{bmatrix} n_1 \\ n_2 \\ n_3 \end{bmatrix} . \tag{6}$$

For example, by transforming the micro-stress vector of the plane 1 to the macro level, we reach to the following six components vector

$$\hat{\sigma}_1 = \frac{1}{6} \begin{Bmatrix} 2\left(\sigma_x + \tau_{xy} + \tau_{xz}\right) \\ 2\left(\sigma_y + \tau_{xy} + \tau_{yz}\right) \\ 2\left(\sigma_z + \tau_{zy} + \tau_{xz}\right) \\ \sigma_x + \sigma_y + 2\tau_{xy} + \tau_{yz} + \tau_{xz} \\ \sigma_y + \sigma_z + \tau_{xy} + 2\tau_{yz} + \tau_{xz} \\ \sigma_x + \sigma_z + \tau_{xy} + \tau_{yz} + 2\tau_{xz} \end{Bmatrix} . \tag{7}$$

By summing up the transformed six component vectors according of their weighting functions, we obtain

$$\sum_{p=1}^{26} W_p \hat{\sigma}_P = \frac{1}{3} \begin{Bmatrix} \sigma_x & \sigma_y & \sigma_z & \tau_{xy} & \tau_{yz} & \tau_{zx} \end{Bmatrix}^T , \tag{8}$$

where the subscript p denotes any specified micro-plane.

As a general rule for the numerical integration of an arbitrary function $f(x,y,z)$ over the surface of unit sphere, we can use the following 26 sampling point equations

$$\int_{\Omega} f(x,y,z)\, d\Omega = 4\pi \sum_{p=1}^{26} W_p f(x_p, y_p, z_p). \tag{9}$$

Comparing equations (8) and (9) we can write

$$\int_{\Omega} \mathbf{T}.\boldsymbol{\sigma} : N\, d\Omega = \int_{\Omega} \hat{\boldsymbol{\sigma}}\, d\Omega = 4\pi \sum_{p=1}^{26} W_p \hat{\sigma}_p = \frac{4\pi}{3} \left\{\sigma_x\ \sigma_y\ \sigma_z\ \tau_{xy}\ \tau_{yz}\ \tau_{zx}\right\}^T. \tag{10}$$

So, in order to obtain the original stress tensor we can write the equation

$$\sigma_{ij} = \frac{3}{4\pi} \int_{\Omega} \left(\sigma_N.N_{ij} + \sigma_M.M_{ij} + \sigma_L.L_{ij}\right)\, d\Omega, \tag{11}$$

$$\sigma_{ij} = 3 \sum_{p=1}^{26} W_p \left(\sigma_N.N_{ij} + \sigma_M.M_{ij} + \sigma_L.L_{ij}\right) =$$

$$= 6 \sum_{p=1}^{13} W_p \left(\sigma_N.N_{ij} + \sigma_M.M_{ij} + \sigma_L.L_{ij}\right). \tag{12}$$

This comparison shows that the pre-multiplier in equations (12) and (1) for superimposition is not the same hence it is not correct.

Furthermore, it is worth noting that in the static constraint approach, the equilibrium of the forces at a point are satisfied automatically because of the projection of the stress tensor to the planes, but the compatibility condition of strain tensor is met only in particular cases. In other words, the micro-strain components acting on the planes may not be always the projection of the strain tensor, because the way of the superimposition of micro-strain components which are used in the static constraint approach (relation (1)) does not guarantee to be the same as the summation of the projections of macro-strain tensor obtained on every plane.

3. A NOVEL MICRO-PLANE DAMAGE FORMULATION

After the above argument which has been done about the theory of the micro-plane approach, in this section we present a new formulation of the

micro-plane model in the area of damage theory which is going to be applied for the simulation of the behavior of the plane concrete. This formulation has some specifications distinct from the other micro-plane damage models.

In order to satisfy both the static equilibrium and compatibility conditions, we have considered a new method of projecting the stress tensor to the micro-planes as described earlier in this article. Then, we derived the strain tensor in terms of the stress tensor based on a well-capable constitutive relation in an ordinary three-dimensional coordinate system. In the second case, the derived strain tensor was projected to or transformed on the micro-planes. So, at this stage, by comparing the components of the stress and strain on the micro-planes we must be able to define the equal microscopic constitutive relations in such a way that both the stress and strain components on each micro-plane are the projections of the corresponding stress and strain tensors. In fact, this situation is the double constraint formulation in which the equilibrium of forces and compatibility of displacements in every integration points are satisfied one by one.

In order to attain the double constraint aspect, after analogy of the projections of stress and strain tensors to the micro-planes obtained in the manner that was explained in the previous section, it was certain that it is necessary to separate the behavior of the material into two distinct parts namely as deviatory and volumetric. So, if firstly we discretize the strain tensor as the volumetric and deviatory parts and then project each of them to the micro-planes separately, we may try to obtain the deviatory part of the modules matrix from the behaviors on the micro-planes whereas the volumetric one, which is not affected by the direction characteristics and essentially is isotropic, is obtained in the ordinary coordinate system and summed up to the deviatory part at the end of each step of loading. Therefore, we can write

$$D_{ijkl} = \frac{3}{4\pi}\int_{\Omega}\left(\frac{E}{1+\nu}\right)\left[\left(N_{ij}-\frac{\delta_{ij}}{3}\right)\left(N_{kl}-\frac{\delta_{kl}}{3}\right)+M_{ij}M_{kl}+L_{ij}L_{kl}\right]d\Omega+$$

$$+\frac{E}{1-2\nu}\frac{\delta_{kl}}{3}\delta_{ij}. \tag{13}$$

4. NEW ANISOTROPY DAMAGE FUNCTION FORMULATION

The total deviatory part of constitutive matrices is computed from superposition of its counterparts on the micro-planes. In turn, these counterparts are calculated based on the damages occurred on each plane depending on its specific loading conditions. This damage is evaluated according to the five separate damage functions; each of them belongs to the particular loading states. This five loading conditions are

1) hydrostatic compression, 2) hydrostatic extension, 3) pure shear, 4)shear + compression, 5)shear + extension.

On each micro-plane, at each time of loading history, there exists one specific loading situation that may be in one of the five mentioned basic loading conditions. For every five mood, a specific damage function according to the authoritative laboratory test results available in the literature is assigned. Then, for each state of on-plane loading, one of the five introduced damage functions will be computed with respect to the history of micro-stress and strain components.

In this formulation we consider just two basic material parameters for ease as elasticity and Poisson's coefficients.

5. UNIAXIAL COMPRESSION (UC) TEST

As can be seen in fig. 4, there is a good agreement between the results obtained by using the proposed model and experimental evidences. The material parameters used in the above analysis are: $E = 25000\,MPa$, $\nu = 0.20$.

In fig. 5, the volumetric changes of the concrete specimen under uniaxial compressive loading have been compared with the experimental observations experienced by Kupfer and his co-workers in 1969. As it is shown, there exists an excellent coincidence between analytical and laboratory data.

In order to show more confidence on the capability of the micro-planes during uniaxial compression test, in figs. 6 - 11, the variation of micro-stress normal and tangential component values are represented versus the total axial compressive stress. It can be seen that, during the application of the uniax-

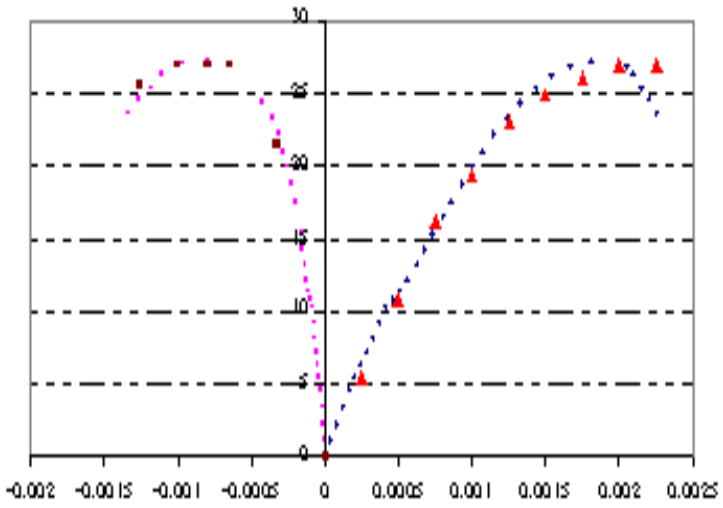

Fig. 4. Axial and lateral strains in mm/mm (right and respectively left horizontal semi-axis) versus axial stress in MPa (vertical axis) in uniaxial compression test of concrete obtained by means of the proposed micro-plane damage model ($f_c' = 27MPa$); red triangles at right and black squares at left represent experimental data from Kupfer et al., 1969.

ial compressive load on the x-axis, the micro-plane number 11 is under just the compressive stress, whereas the micro- planes numbers 9,10,12,13, which geometrically are located normal to the load direction on the unit sphere, are only under the tensile stress. The compressive stress accompanied with shear affects the other remaining planes. During the increase of the uniaxial compressive load, the compressive and shear stress components acting on the micro-planes number 1 to 8 first increase together with the shear stress, but near the peak stress (f_c'), the compressive stress decreases suddenly.

Fig. 12 shows the growth of the damage function values of different micro-planes during uniaxial compression test of concrete obtained with the proposed model. Namely, the damage evolutes on the micro-planes number 9,10,12,13 on the unit sphere faster than the other planes. This is due to the existence of different modes of loading on those planes. In the uniaxial compression test done by the proposed model, the axial compressive load is applied to the x-axes that are normal to the micro-plane number 11. So, on this plane, there exists only a normal compressive load (mode I) for which no damage could

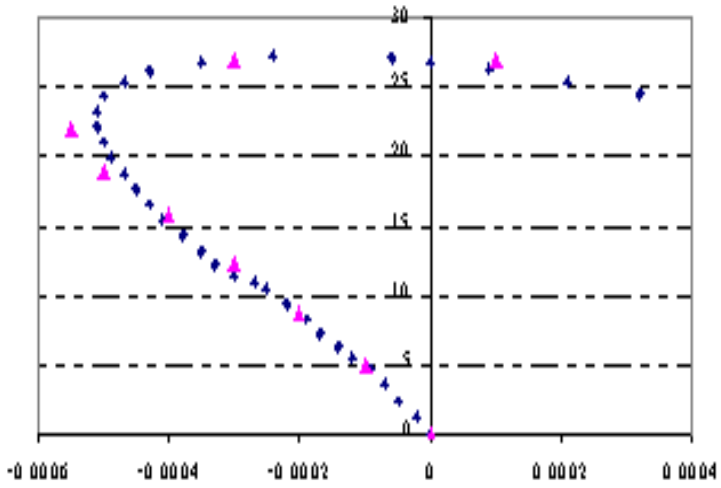

Fig. 5. Volumetric behavior of concrete (on the horizontal axis - compression at the left, dilation at the right of 0) under uniaxial compressive loading (on the vertical axis); violet triangles represent experimental data from Kupfer et al., 1969 ($f'_c = 27MPa$).

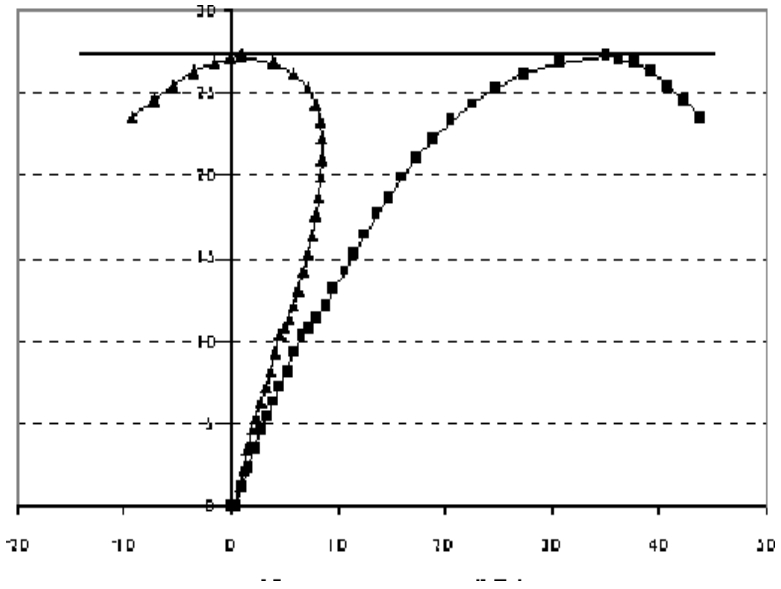

Fig. 6. Variation of micro stress components acting on the micro planes number 1,2,3,4 during uniaxial compression test. On the horizontal axis - the micro stress components (MPa), on the vertical axis - axial compressive stress; the left branch - normal component, the right branch - tangential component.

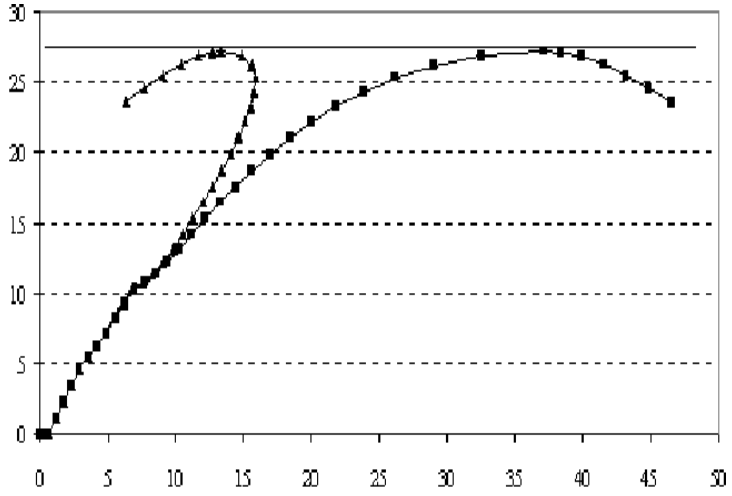

Fig. 7. Variation of micro stress components acting on the micro planes number 5, 6 during uniaxial compression test. On the horizontal axis- the micro stress components (MPa), on the vertical axis- axial compressive stress (MPa); the left branch - normal component, the right branch - tangential component.

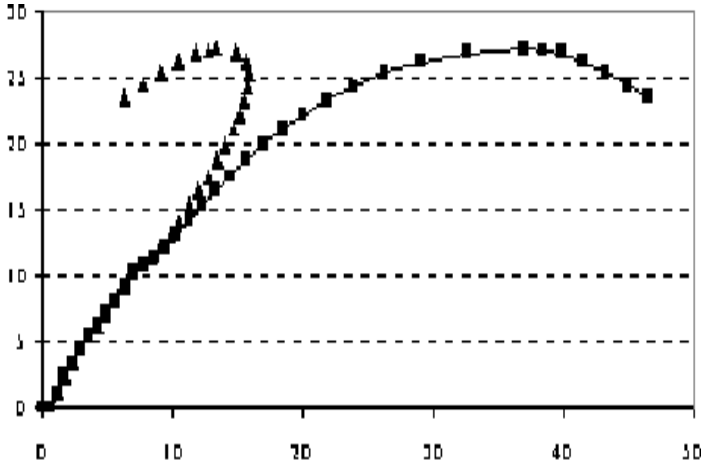

Fig. 8. Variation of micro stress components acting on the micro planes number 7, 8 during uniaxial compression test. On the horizontal axis- the micro stress components (MPa), on the vertical axis- axial compressive stress (MPa); the left branch - normal component, the right branch - tangential component.

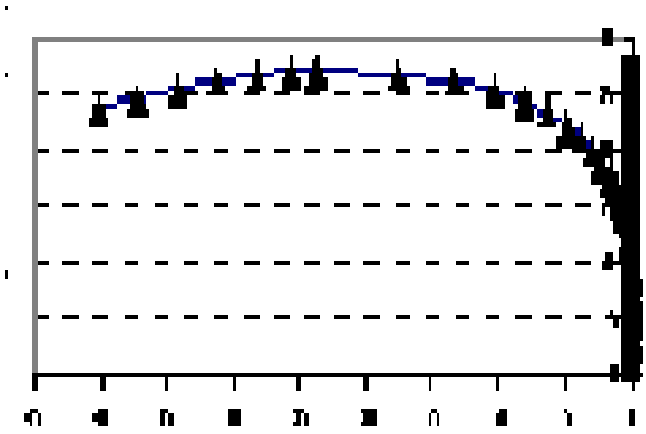

Fig. 9. Variation of micro stress components acting on the micro planes number 9, 10 during uniaxial compression test. On the horizontal axis- the micro stress components (MPa), on the vertical axis- axial compressive stress (MPa); the left branch - normal component, the vertical branch - tangential component.

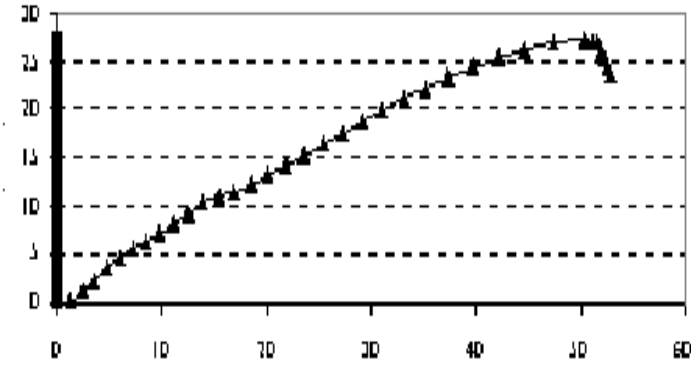

Fig. 10. Variation of micro stress components acting on the micro plane number 11 during uniaxial compression test. On the horizontal axis- the micro stress components (MPa), on the vertical axis- axial compressive stress (MPa); the right branch - normal component, the vertical branch - tangential component.

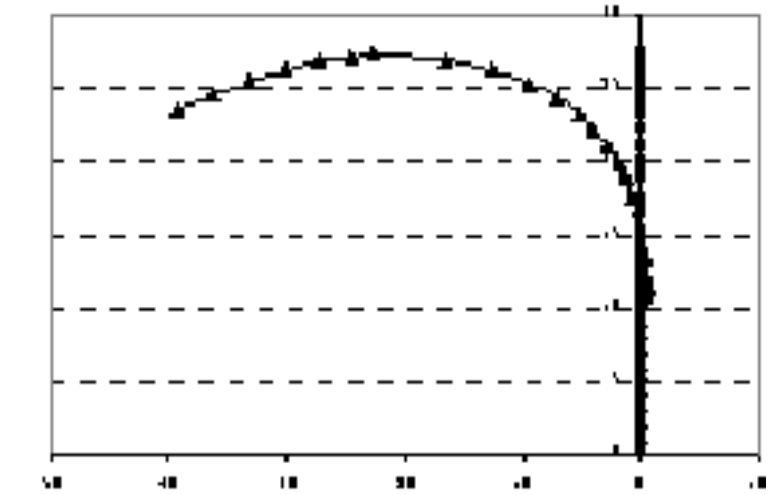

Fig. 11. Variation of micro stress components acting on the micro planes number 12, 13 during uniaxial compression test. On the horizontal axis- the micro stress components (MPa), on the vertical axis- axial compressive stress (MPa); the left branch - normal component, the vertical branch - tangential component.

occur on it. On the micro-planes number 5,6,7,8 there is a shear combined with the normal compressive load (mode IV) causing damages less than the micro-planes 1,2,3,4 on which there exists the same mode of loading (mode III). This is because of the fact that on the micro-planes number 1, 2, 3 and 4 the magnitude of the compressive stress component is less than the same component value on the micro-planes number 5 to 8 (figs. 6- 12), so damage growths faster.

Finally, on the micro-planes number 9,10,12,13 there exists only normal tension loading (mode II), which causes the damage growths faster than the all other planes (figs. 9-11).

From the above behaviors of the micro-planes, obtained by using the proposed model, we conclude that in the uniaxial compression test, the damages or cracks can appear first on the micro-planes number 9,10,12,13 and then on the micro-planes number 1, 2, 3 and 4. This can be observed in the real situation of the laboratory on the cylindrical concrete specimen. If there is no friction restraint between the surfaces of the loading top/bottom plates and

the specimen, then the cracks will appear differently on the positions of the micro-planes number 9,10,12,13 of the proposed model. Else if the damages on the micro-planes number 1, 2, 3 and 4 will be greater and cracks will be initiated first on these planes. As a result, the effect of lateral confining pressures on the compressive cylindrical strength of concrete specimens simulated by the proposed model has been compared with experimental data of Ansari and Li (1998) in fig. 14.

Fig. 15 exhibits the behavior of concrete specimen under conventional triaxial extension (CTE) test that is presented by the proposed model.

6. CONVENTIONAL TRIAXIAL COMPRESSION (CTC) TEST

In this test, at first the hydrostatic pressure is applied to the specimen to a certain level and then the axial compression is increased while the lateral or confining pressure is held constant. So, in this test, up to certain level of hydrostatic compression, there must be no shear forces on the micro-planes. This can be seen in fig. 12 that shows the evolution of the micro-stress components on different micro-planes during CTC test. In fig. 13, the axial stress-strain curves of cylindrical concrete specimen under two different Uniaxial Compression (UC) test and Conventional Triaxial Compression (CTC) test obtained by using the proposed micro-plane damage model have been compared.

The stress-strain response of the concrete cylindrical specimen under UT test that is depicted in fig. 16. In fig. 17 the proposed model prediction under hydrostatic tension (HT) test is depicted. The load capacity of the sample under the hydrostatic tension is greater than the same value in the UT test because in the UT test the cause of the damage is the compromise of tension and shear stress while in the HT test, the pure tensile stress acting on the planes. The prediction of the proposed micro-planes for the HT test is shown in the fig. 18. As it can be noticed, the behavior of all micro-planes under this loading is the same. The reason is that in the hydrostatic loading, the same condition of stress distributions is imposed around the physical point and

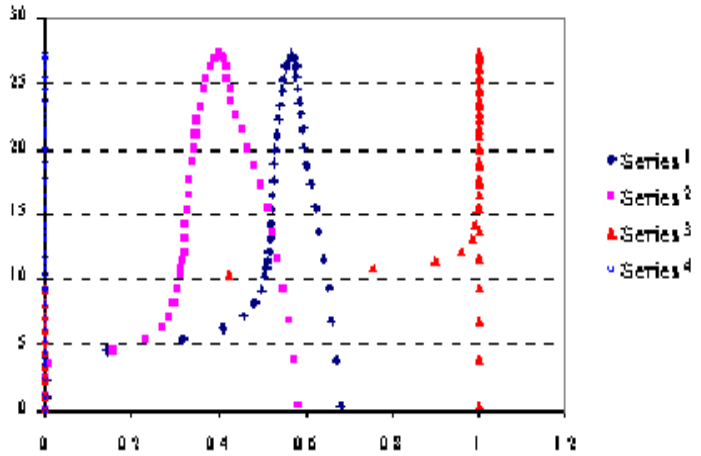

Fig. 12. Comparison of the damage evolution functions on the various micro-planes during the axial compressive loading. On the horizontal axis- the damage evolution function value, on the vertical axis- the axial stress (MPa).

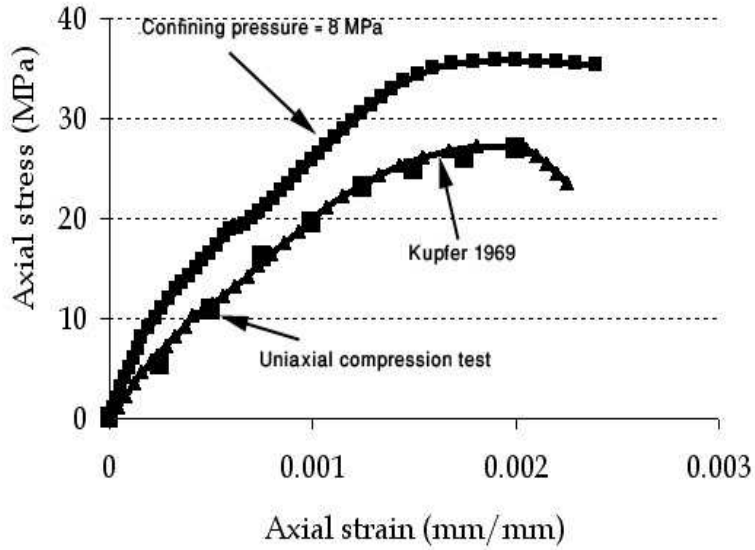

Fig. 13. Comparison of axial stress-strain curves of concrete in UC and CTC tests.

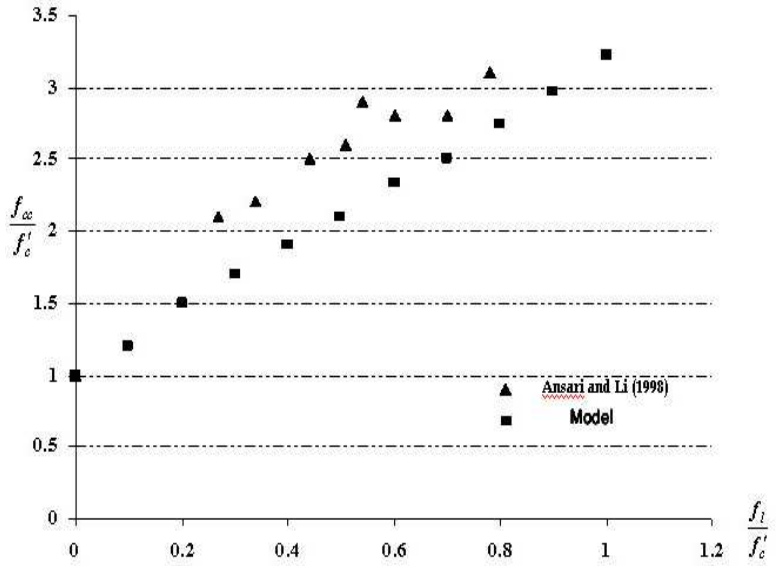

Fig. 14. Different triaxial compression strengths f_{cc} obtained for different lateral confining pressures f_l.

therefore the anisotropy could not appear. Furthermore, as it is anticipated, there is no shear stress on the planes.

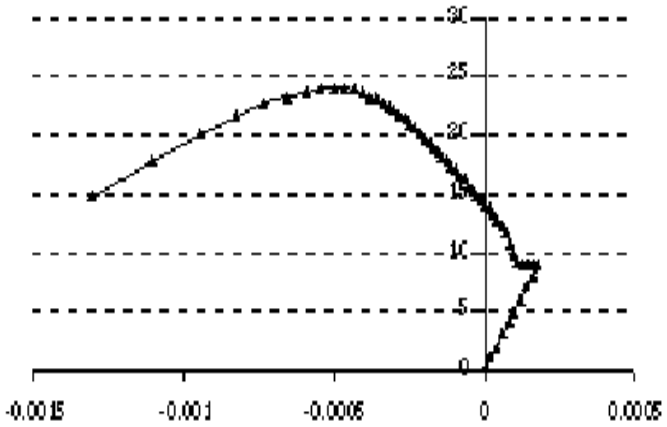

Fig. 15. Behavior of the cylindrical concrete specimen under (CTE) test obtained by using the proposed micro-plane damage model.

The expected response of concrete cylindrical specimen under hydrostatic compression (HC) test, associated with the increase of bearing capacity unlimitedly. Simulation of this response under the HC test is presented in fig. 19, 20. As in the case of HT test, the behavior of the whole planes under the HC test is the same.

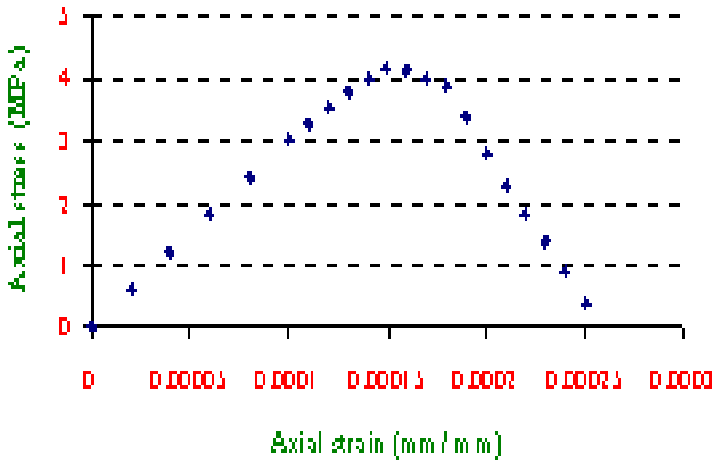

Fig. 16. Behavior of the cylindrical concrete specimen under uniaxial tension test obtained by using the proposed micro-plane damage model.

7. CYCLIC LOADING

Generally, the most damage models fail to reproduce the irreversible strains and the slopes of the curve in the unloading and reloading regions.

In fig.21, the predicted response of the model under cyclic compression test is compared with the experimental results of B. P. Sinha, K. H. Gerstle and L. G. Tulin (1964). A good agreement between the analytical and experimental data is seen. Also, in fig. 22, the behavior of concrete simulated by using the proposed model under complete cyclic loading is shown.

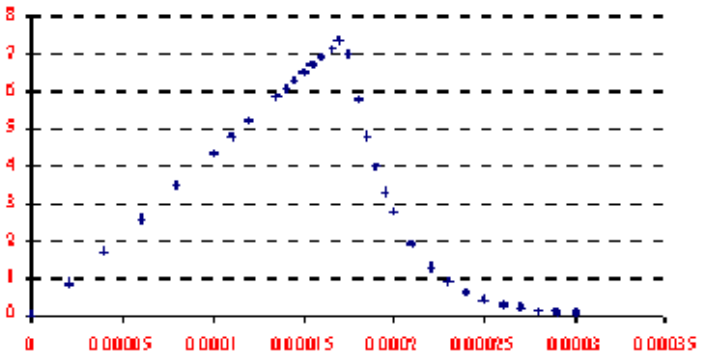

Fig. 17. Behavior of the cylindrical concrete specimen under HT test obtained by using the proposed micro-plane damage model; axial strain (mm/mm) - on the horizontal axis, axial tensile stress (MPa) - on the vertical axis.

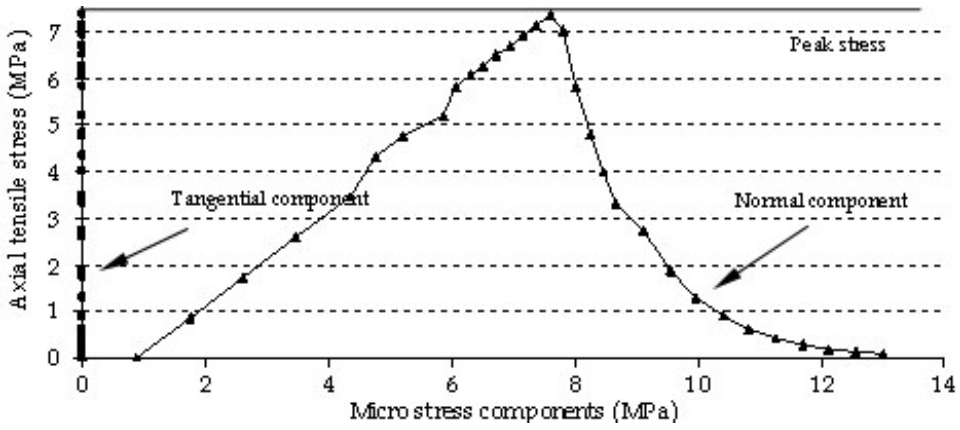

Fig. 18. Variation of micro-stress component values acting on the micro-planes number 1 to 13 during the HT test.

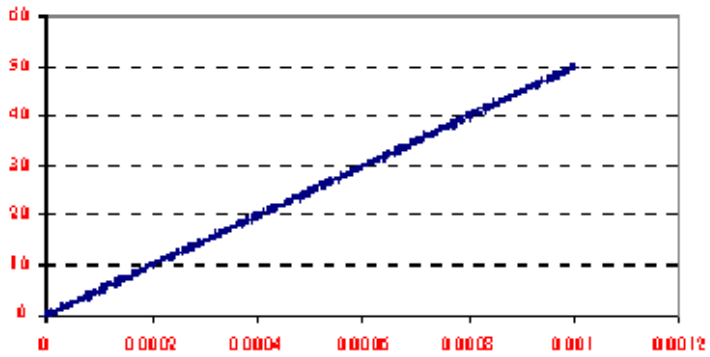

Fig. 19. Behavior of the cylindrical concrete specimen under the HC test obtained by using the proposed micro-plane damage model; axial strain (mm/mm) - on the horizontal axis, axial tensile stress (MPa) - on the vertical axis.

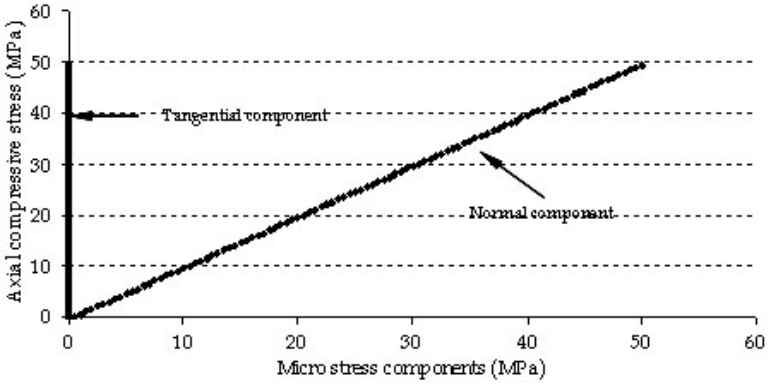

Fig. 20. Variation of micro-stress component values acting on the micro-planes number 1 to 13 during the HC test.

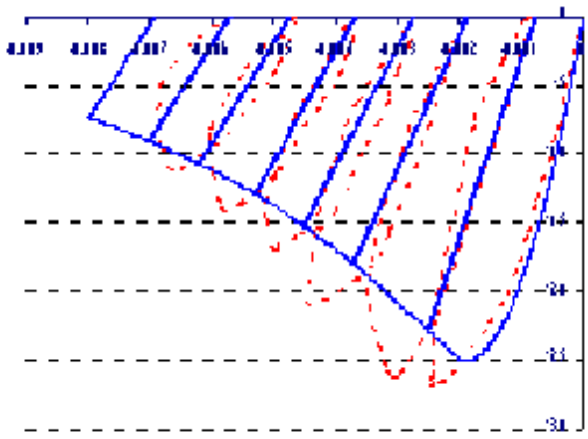

Fig. 21. Cyclic compression test simulation; axial strain (mm/mm) on the horizontal axis, axial stress (MPa) on the vertical axis, blue continuous line - proposed model, red dotted line- experimental results.

8. CONCLUSIONS

A constitutive damage model for the mechanical behavior of concrete/rock under arbitrary loadings was developed using the composition of the theoretical framework of micro-plane and damage approaches. A new damage formulation has been employed into the micro-plane model. Accordingly, an arbitrary change of six strain/stress on cube element led to combination of five conditions introduced on plane. Therefore, the proposed model is capable of predicting the concrete behavior under an arbitrary strain/stress path. These five force conditions are: *1)hydrostatic compression, 2)hydrostatic extension, 3)pure shear, 4)shear + compression, 5)shear + extension.* The five damage evolution functions, all of them functions of equivalent strain, were formulated for any of the five force conditions. This novel micro-plane damage model can simulate the behavior of the concrete/rock specimen under compressive loadings as well as tensile loadings with a few model parameters requirements. The proposed model has excellent features, such as prefailure configuration of inside material, final failure mechanism, capability of seeing induced/inherent anisotropy and also any fabric effects on the material behavior. However, the

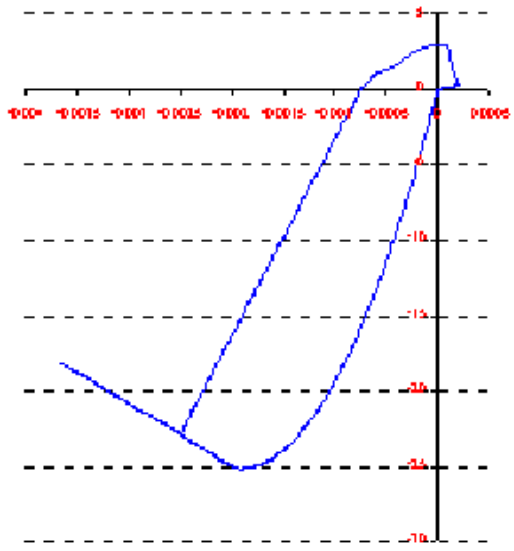

Fig. 22. Complete cyclic test simulation; axial strain (mm/mm) on the horizontal axis, axial stress (MPa) on the vertical axis (the sense on the cycle is clockwise).

basis of its formulation is simple, logical and has some physical insights that make it convenient to perceive.

References

[1] Batdorf, S. B., Budiansky, B., *A mathematical theory of plasticity based on the concept of slip*, Technical Note **1871**, National Advisory Committee for Aeronautics, 1949.

[2] Ramm, E., D'Addetta, G. A., Leukart, M., *From microscopic to macroscopic modeling of geomaterials*, European Congress on Computational Methods in Applied Sciences and Engineering, 2004.

[3] Bazant, Z.P., Gambarova, P.G., *Crack shear in concrete: Crack band micro plane model*, J. Struct. Eng., ASCE, **110**(1984), 2015-2036.

[4] Bazant, Z., Oh, B., *Micro plane model for progressive fracture of concrete and rock*, J. E. Mech., **111**(1985), 559-582.

[5] Bazant, Z., Prat, P., *Micro plane model for brittle plastic material: Part I & II*. J. E. Mech., 114, pp.1672-1702, 1988.

[6] Carol, I., Bazant, Z., *Damage and plasticity in micro plane theory*, Int. J. Solids & Structures., **34**(1997), 3807-3835.

[7] Carol, I., Bazant, Z. P., Prat, P., *New explicit microplane model for concrete: Theoretical aspects and numerical implementation*, Int. J. Solids & Structures, **29**(1992), 1173-1191.

[8] Carol, I., Jirasek, M., Bazant, Z. P., *A thermodynamically consistent approach to micro plane theory. Part I: Free energy and consistent micro plane stresses*, Int. J. Solids & Structures, **38**(2001), 2921-2931.

[9] Kuhl, E., Ramm, E., de Borst, R., *An anisotropic gradient damage model for quasi-brittle materials*, Comp. Meth. Appl. Mech. Eng., **183**(2000), 87-103.

[10] Kuhl, E., Ramm, E., *Micro plane modeling of cohesive frictional materials*, Eur. J. Mech." A/Solids, **19**(2000), S121-S143.

[11] Simo, J., Ju, J., *Strain and stress based continuum damage models: Part I-Formulation, Part II-Computational aspects*, Int. J. Solids and Structures **23**(1987), 821-869.

[12] Bazant, Z. P., Adley, M. D., Carol, I., Jirasek, M., Akers, S.A., Rohani, B., Cargile, J.D., Caner, F.C., *Large-strain generalization of micro plane constitutive model for concrete and application*, ASCE, J. Engrg. Mech. 126(9)(2000a), 971-980.

[13] Bazant, Z. P., Caner, F. C., Carol, I., Adley, M.D., Akers, S.A., *Micro plane model M4 for concrete: I. Formulation with work-conjugate deviatoric stress*, ASCE, J. Engrg. Mech. **126**(9)(2000b), 944-953.

[14] Bazant, Z. P., Caner, F. C., *Micro plane M4 for concrete: II. Algorithm and calibration*, ASCE, J. Engrg. Mech. **126**(2000), 954-961.

[15] Ozbolt, J., Li, Y., Kozar, I., *Micro plane model for concrete with relaxed kinematic constraint*, Int. J. Solids Struct., **38**(2001), 2683-2711.

[16] Pijaudier-Cabot, G., Bazant, Z. P., *Non local damage theory*, J. Engrg. Mech. ASCE, **113**(1987), 1512-1533.

[17] Mazars, J., *A description of micro and macro scale damage of concrete structures*, J. Engrg. Fracture Mech., **25**(1986), 729-737.

[18] Meschke, G., Lackner, R., Mang, H., *An anisotropic elastoplastic-damage model for plane concrete*, Int. J. Numerical Methods in Engrg., **42**(1998), 703-727.

[19] Yazdani, S., Schreyer, H.L., *An anisotropic damage model with dilatation for concrete*, Mechanics of Materials **7**(1988), 231-244.

[20] Lubarda, V. A., Krajcinovic, D., *Damage tensor and the crack density distribution*, Int. J. Solids Structures, **30**(20)(1993), 2859-2877.